Targeting of Histone Acetyltransferase p300 by Cyclopentenone Prostaglandin Δ^{12}-PGJ$_2$ through Covalent Binding to Cys^{1438}

Kodihalli C. Ravindra[†], **Vivek Narayan**[†], **Gerald H. Lushington**[‡], **Blake R. Peterson**[‡], and **K. Sandeep Prabhu**[*,†]

[†]Center for Molecular Toxicology and Carcinogenesis and Center for Molecular Immunology and Infectious Disease, Department of Veterinary and Biomedical Sciences, The Pennsylvania State University, University Park, Pennsylvania 16802, United States

[‡]Department of Medicinal Chemistry, The University of Kansas, Lawrence, Kansas 66045, United States

Abstract

Inhibitors of histone acetyltransferases (HATs) are perceived to treat diseases like cancer, neurodegeneration, and AIDS. On the basis of previous studies, we hypothesized that Cys^{1438} in the substrate binding site could be targeted by Δ^{12}-prostaglandin J$_2$ (Δ^{12}-PGJ$_2$), a cyclopentenone prostaglandin (CyPG) derived from PGD$_2$. We demonstrate here the ability of CyPGs to inhibit p300 HAT-dependent acetylation of histone H3. A cell-based assay system clearly showed that the α,β-unsaturation in the cyclopentenone ring of Δ^{12}-PGJ$_2$ was crucial for the inhibitory activity, while the 9,10-dihydro-15-deoxy- Δ^{12,14}-PGJ$_2$, which lacks the electrophilic carbon (at carbon 9), was ineffective. Molecular docking studies suggested that Δ^{12}-PGJ$_2$ places the electrophilic carbon in the cyclopentenone ring well within the vicinity of Cys^{1438} of p300 to form a covalent Michael adduct. Site-directed mutagenesis of the p300 HAT domain, peptide competition assay involving p300 wild type and mutant peptides, followed by mass spectrometric analysis confirmed the covalent interaction of Δ^{12}-PGJ$_2$ with Cys^{1438}. Using biotinylated derivatives of Δ^{12}-PGJ$_2$ and 9,10-dihydro-15-deoxy- Δ^{12,14}-PGJ$_2$, we demonstrate the covalent interaction of Δ^{12}-PGJ$_2$ with the p300 HAT domain, but not the latter. In agreement with the *in vitro* filter binding assay, CyPGs were also found to inhibit H3 histone acetylation in cell-based assays. In addition, Δ^{12}-PGJ$_2$ also inhibited the acetylation of the HIV-1 Tat by recombinant p300 in *in vitro* assays. This study demonstrates, for the first time, that Δ^{12}-PGJ$_2$ inhibits p300 through Michael addition, where α,β-unsaturated carbonyl function is absolutely required for the inhibitory activity.

[*]Corresponding Author: Tel: 814-863-8976. ksprabhu@psu.edu.

Introduction

The action of cyclooxygenase (COX) enzymes on arachidonic acid, followed by isomerization of the product PGH_2 by hematopoietic PGD synthase (H-PGDS) or lipocalin PGDS (L-PGDS) leads to the formation of PGD_2, which undergoes dehydration to form PGJ_2, Δ^{12}-PGJ_2, and 15d-PGJ_2.[1] Because the latter set of metabolites have a conserved cyclopentenone structure, these molecules are commonly referred to as CyPGs of the J_2 class. These CyPGs are implicated in a wide variety of diverse functions, such as anti-inflammatory, antiviral, antitumor, and cytoprotective effects via multiple mechanisms, including the modulation of transcription factors such as NF-κB, Nrf-2, and PPARγ.[2–8] Recently, we have demonstrated the essential role of selenoproteins in the expression of H-PGDS leading to enhanced production of CyPGs.[3] Interestingly, CyPGs interact covalently with the nucleophilic Cys thiolate anion in proteins via the two electrophilic carbons at positions 9 and 13.[9–12] CyPGs form Michael adducts with nucleophiles such as the free sulfhydryl group of Cys residues located in reduced glutathione (GSH) or many cellular proteins, including thioredoxin, p50, Ras, p53, Keap-1, IKK2, and HIV-1 Tat.[4,7,9,13–19] As a result, modification of functionally important sulfhydryl groups in many proteins often results in the modulation of their biological activities, leading to changes in the transcription of several downstream gene targets.[20]

The DNA is packaged as chromatin in the nucleus of eukaryotes by both histone and nonhistone proteins.[21] Chromatin plays a pivotal role in transcription, DNA repair, and replication.[22,23] The basic unit of chromatin is the nucleosome, which is composed of dimers of histones H2A, H2B, H3, and H4 around which 147 base pairs of DNA are wrapped. The N-terminal tails of histones are exposed to the surface of the nucleosome, which serve as the main sites for post-translational modifications. Among the different post-translational modifications, reversible acetylation of histones plays an important role in maintaining the structure of the chromatin.[24,25] Therefore, histone acetylation plays an essential role in epigenetic regulation. Histone acetyltransferases (HATs) refers to the class of enzymes that catalyze the acetylation reaction, which transfers the acetyl group from acetyl-CoA to the amino tail of histones and other proteins at specific lysine residues. Thus, HATs are also referred to as lysine acetyltransferases (KATs). These enzymes and the associated acetylation events have been implicated in a wide variety of physiological and diseases like neurodegeneration, cancer, HIV-AIDS, and inflammation.[26–29] Histone acetylation is catalyzed by five different classes of HATs.[30] Among them, the best studied are p300 (also referred to as KAT3B) and its close analogue CBP (KAT3A).

Histone acetyltransferase p300 is involved in various cellular events, and its dysfunction is linked to diseases like cancer.[27] The increasing evidence of p300 HAT activity with cancer causation and progression has made it to be targeted for the development of anticancer therapeutics. Many of the inhibitors of these enzymes are peptide conjugates of CoA or natural products and their derivatives.[31–36] All these inhibitors provide a valuable tool for analyzing the structure and function of these enzymes, although their potential for development as clinical drug candidates still remains to be determined. However, given the presence of Cys^{1438} in the substrate-binding site of p300 HAT domain that is critical in the binding and stabilization of the substrate, we hypothesized that CyPGs are likely to target this reactive Cys residue to inhibit the enzymatic activity of p300.[37,38]

In this study, we describe the ability of CyPGs to inhibit the activity of p300 *in vitro* and in hepatocytes and macrophages. Our studies comparing the various CyPGs clearly evolve an intriguing structure–activity relationship in PGs indicating the importance of the *α,β*-unsaturated carbonyl function to be essential to inhibit the activity of p300 HAT. Molecular

modeling studies, showing the interaction of biotinylated derivatives of CyPGs, further lend credence to the idea that these reactive metabolites could impact epigenetic and gene regulatory functions. Here, we also provide data to translate these findings to address the inhibitory role of Δ^{12}-PGJ$_2$ in the p300-dependent activation of a critical HIV transcriptional activator, Tat.

Experimental Procedures

Materials

The following PGs were purchased from Cayman Chemicals (MI, USA): Δ^{12}-PGJ$_2$, PGJ$_2$, PGD$_2$, PGE$_2$, PGK$_2$, PGA$_2$, PGB$_2$, 9,10-dihydro-15d-PGJ$_2$, and 13,14-dihydro-PGD$_2$. All compounds were of high purity and were used without further purification. [Acetyl-1-^{14}C]-CoA (60 mCi/mmol) was purchased from Perkin-Elmer Life Sciences (Waltham, MA). Whatman P81 chromatography paper was obtained from Fisher Scientific Chemicals (Pittsburgh, PA). HeLa core histones and antibodies that recognize specific acetylated lysine residues in histone H3 (K9 and K14) and total histone H3 were obtained from Active motif (Carlsbad, CA). GST-tagged recombinant p300 HAT domain corresponding to amino acids 1066–1707 of human p300 expressed in *E.coli* was obtained from Millipore (Billerica, MA). Similarly, GST-tagged recombinant PCAF (p300/CBP-associated factor; 165 amino acids; corresponding to residues 503–651) was purchased from Cayman Chemicals. HIV-1 Tat protein was expressed in a bacterial system and purified using His-affinity chromatography in our laboratory as described previously.[14]

Histone Acetyltransferase Assay

HAT assays were performed as described previously with some modifications.[39] p300 or PCAF were incubated with or without molar equivalents of PGs at room temperature for 3 h. Then 0.8 μg of highly purified HeLa core histones were incubated in HAT assay buffer (50 mM Tris–HCl, pH 8.0, 1 mM PMSF, 0.1 mM EDTA, and 10% v/v glycerol) at 30 °C for 10 min, with or without p300 or PCAF (PG treated and untreated). The reaction mixture was incubated for an additional 10 min upon addition of 0.25 μL of 60 mCi/mmol ^{14}C acetyl CoA in a total volume of 30 μL. The reaction mixture was then blotted onto a P-81 filter paper (Whatman) and washed with carbonate buffer (0.2 M Na$_2$CO$_3$ and 0.2 M NaHCO$_3$), and counts were recorded in a Beckman liquid scintillation counter. All assays were performed in triplicate.

Viability Assay

All PGs were tested for toxicity at 10 μM. The viability of cells after various treatments was estimated in terms of their ability to reduce the dye (3,4,5- dimethyl thiazol-2-yl)-2,5-diphenyl tetrazolium bromide (CCK-8 kit, Dojindo, Gaithersburg, MD) to blue purple formazan crystals, as per the manufacturer's instructions.

Analysis of Histone Acetylation in HepG2, RAW264.7, and U1/HIV-1 Cells

Human liver hepatoblastoma (HepG2) cells (ATCC; HB-8065) (1×10^6 cells per 60 mm^2 dish) were seeded overnight and treated with various PGs at indicated concentrations or vehicle (DMSO, 0.1% v/v) the following day for 24 h. Murine macrophage-like cells (RAW264.7; ATCC) were cultured in Dulbecco's minimum essential medium containing D-glucose (5 mM; Invitrogen), sodium selenite (250 nM; Sigma Aldrich), and FBS (5%, v/v; ATCC). These cells were stimulated with *E. coli* LPS (50 ng/mL) for 2 h and cultured in the above media in the presence or absence of indomethacin (10 μM) or HQL-79 (25 μM; Cayman), which inhibit COX-1/2 and H-PGDS, respectively. Total histones were extracted from vehicle and compound-treated cells as described previously.[35] Equal amounts of the

protein samples were run on a 12% (%T) SDS–polyacrylamide gel and the separated histones were electro-transferred onto a nitrocellulose membrane. The membranes were probed with specific anti-(K9/K14) acetyl H3 and total anti-H3 C-terminal antibodies (Active motif). Detection was performed with goat antirabbit secondary antibody (Thermo Pierce, Rockford, IL), and bands were visualized using the ECL detection system (Thermo Pierce). U1/HIV-1 cells, obtained from the NIH AIDS Research and Reference Reagent Program, were cultured in RPMI 1640 supplemented with FBS (10% v/v) and stimulated for 12 h with 20 ng/mL phorbol myristic acid (PMA; Sigma) and subsequently treated with vehicle or Δ^{12}-PGJ$_2$ for 24 and 48 h. Histones were isolated from the cells, and their acetylation status was analyzed as described earlier.

Site-Directed Mutagenesis of the p300 HAT Domain

The p300 HAT cDNA (region corresponding to amino acid residues 1066 to 1707) was cloned from HEK293T cDNA using the following primers: forward, 5′ TACCGTCAGGATCCAGAATCCCTTCCC 3′, and reverse, 5′ TTTCTCCATTTTGTGGTCATGGTTTTTAGTGTTATAGC 3′. *Eco*RI and EagI restriction endonuclease sites (in bold) were added to the p300 cDNA using the primers forward, 5′ **GAATTC**TACCGTCAGGATCCAGAATCC 3′, and reverse, 5′ CCATAGC**GGCCGC**TTTCTCCATTTTGTGGTCATGG 3′. The p300 cDNA was subcloned into *Eco*RI and EagI sites in the pET41c(+) vector (Novagen). Such a pET41c-p300 plasmid was used as the template to generate the p300C1438A mutant using the Stratagene site-directed mutagenesis kit according to the manufacturer's instructions. The primers used for the mutagenesis were as follows: forward, 5′ GCATATTTGGGCA**GCA**CCACCAAGTGAG 3′; and reverse, 5′ CCTCACTTGGTGG**TGC**TGCCCAAATATG 3′ (underlined codons in bold represent the mutated Cys residue).

Reaction of the p300 HAT Domain and Biotinylated PGs

The ability of these compounds to bind the p300 HAT domain was examined *in vitro*. Δ^{12}-PGJ$_2$ and 9,10-dihydro-15-deoxy-$\Delta^{12,14}$-PGJ$_2$ were biotinylated using EZ-link-5-(biotinamido)pentylamine (Thermo Pierce) in the presence of EDC (1-ethyl-3-(3-diaminomethylamino-propyl) carbodiimide hydrochloride) as the coupling agent as described.[14] Briefly, the biotinylated PGs were purified on a preparative silica gel 60 column (70–230 mesh; Sigma Chemicals, St. Louis, MO) developed with ethyl acetate followed by elution with ethyl acetate/methanol (80:20). The eluates were run on a thin layer chromatography using AL SILG/UV plates (Whatman, 250 μm layer; Kent, UK). Fractions containing biotinylated PGs were pooled and confirmed by mass spectrometry (*m/z* of 645.44 and 627.78 for Δ^{12}-PGJ$_2$-biotinamide and 9,10-dihydro-15d-PGJ$_2$-biotinamide, respectively) and a dot blot probed with streptavidin-HRP. The p300 HAT domain (10 pmol/30 μL reaction volume), biotinylated Δ^{12}-PGJ$_2$ (10 pmol), and 9,10-dihydro-PGJ$_2$ (10 pmol) were incubated in HAT assay buffer for 3 h (at 25 °C) with 10 μg of cell nuclear extract from U937 monocytic cells. The latter was subjected to pull-down with neutravidin–agarose beads followed by Western blot analysis by with GST antibody or neutravidin–HRP conjugate to examine the interaction between p300 and Δ^{12}-PGJ$_2$.

Binding Studies with C1438A Mutant

BL21 cells were transformed with native pET41c-p300 or pET41c-p300C1438A plasmids. The transformed cells were grown in Terrific Broth to log phase and induced with 1 mM IPTG overnight. Then 0.2 nmol of the native or mutant p300 protein was bound to HisPur resin (Pierce) according to the manufacturer's instructions. Δ^{12}-PGJ$_2$ biotinamide solution (0.2 nmol) prepared in 1% DMSO (in 50 mM Tris-Cl, pH 8.0) was reacted with the resin-bound protein for 3 h at room temperature on an end-to-end shaker. Following washes with

50 mM Tris-Cl, pH 8.0, the resin was boiled with $1\times$ SDS gel loading buffer. HisPur resin alone, 0.2 nmol of Δ^{12}-PGJ$_2$ biotinamide solution bound to resin, native p300, and p300C1438A protein bound to the resin were used as negative controls. The samples were analyzed by Western immunoblotting with the indicated reagents.

Interaction of Δ^{12}-PGJ$_2$ with the p300 Peptide

The peptide sequences [1433]GHIWACPPSEG and its mutant [1433]GHIWAAPPSEG were purchased from GenScript Inc. (Piscataway, NJ). The peptides (0.3 μM) and Δ^{12}-PGJ$_2$ (0.3 μM) were incubated for 3 h in HAT assay buffer, in a reaction volume of 30 μL. The reactions were analyzed by infusion and using an LC-MS/MS system comprising Shimadzu LC20AD UFLC pumps, a Luna phenyl-hexyl column (150 $\times$ 2 mm, 3 μm; Phenomenex), and a ABI2000 triple quadruple mass spectrometer with an electrospray ionization probe set to positive mode at 250 °C for the confirmation of the product ion peak. The solvent system used was methanol/H$_2$O (70:30), with 0.1% acetic acid, at a flow rate 0.15 mL/min.

Peptide Competition Assay

The peptides (10 pmol) were added to the p300 HAT domain (10 pmol) along with biotinylated Δ^{12}-PGJ$_2$ (10 pmol and 20 pmol) for 3 h at 25 °C, in a reaction volume of 30 μL followed by Western blot analysis with neutravidin-HRP or anti-GST.

p24 Quantitation

The U1/HIV-1 cell line was cultured in RPMI-1640 media (Cellgro) supplemented with 10% heat inactivated fetal calf serum (Hyclone), 2 mM L-glutamine (Invitrogen), penicillin (0.5 units/mL), and streptomycin (0.5 μg/mL). The cells were stimulated with 20 ng/mL of PMA for 12 h. Δ^{12}-PGJ$_2$ in DMSO (0.1% v/v) was added to the stimulated cells, and the cultures were incubated at 37 °C for 24 and 48 h. Unstimulated cells were used as a negative control. Culture supernatant was sampled every 24 h for p24 analysis. The quantity of p24 in the samples was measured with a commercial kit following the manufacturer's instructions (CosmoBio, Japan). All of the assays were performed in triplicate.

In Vitro Acetylation of HIV-1 Tat Protein by p300 HAT

Ten picomoles of the p300 HAT domain was incubated in the presence or absence of 30 pmol of Δ^{12}-PGJ$_2$ for 3 h at room temperature in 30 μL. This mixture was then incubated with 350 pmol of His-tag labeled recombinant Tat (rTat) protein and 0.1 μCi of [acetyl-1-^{14}C] CoA for 1 h at room temperature. The rTat protein was subjected to pull-down using HisPur resin, which was boiled, centrifuged, and the supernatant subjected to scintillation counting.

Molecular Docking Studies

To develop a prospective pharmacophore for ligand interactions with the Cys[1438] of p300 HAT domain, we applied a two-stage modeling protocol. First, we docked the following three fragment species: (a) 4-allyl-5-methylenecyclopent-2-enone, (b) (4R,5R)-4-methyl-5-vinylcyclopentane-1,3-dione, and (c) (R)-3-allyl-2-methylenecyclopentanone into p300-HAT via the Surflex program, as guided by specifying a protomol construct based solely on the position and character of Cys[1438] (residue-based protomol generated automatically in Surflex according to default parameters). Docking proceeded according to default parameter settings with the exception that the number of initial starting conformations was increased to 20, and the number of requested poses was set to 50. From the resulting docking simulation, the bound conformations were examined in order to find the top scoring pose that positioned either a sp2 hybridized ring carbon or oxygen within 4 Å of the Cys sulfur; in each case, either the very highest or the second highest scoring pose satisfied this criterion. The

fragment poses selected in this first stage were then merged into a single MOL2 file to serve as the base for a ligand-based protomol generation (performed automatically in Surflex according to default parameters) for the second stage. In the second stage, PGJ_2, Δ^{12}-PGJ_2, PGK_2, and 9,10-dihydro-15-deoxy-$\Delta^{12,14}$-PGJ_2 were docked to p300-HAT via Surflex via the above fragment-based protomol and according to the same docking protocol as described in the first stage. Bound conformations were again examined to identify the top scoring pose that positioned either an sp2 hybridized ring carbon or oxygen as described earlier. This spatial orientation criterion was again satisfied either by the single top scoring pose (as was the case for PGJ_2, PGK_2, and 9,10-dihydro-15-deoxy-$\Delta^{12,14}$-PGJ_2) or by the second-best pose (Δ^{12}-PGJ_2). Pose clustering analysis revealed that the single most populous conformational family resolved for each ligand corresponded to poses satisfying the Cys[1438] spatial proximity criterion, and in each case, more than half of all poses placed either the ring oxygen or electrophilic carbon within a somewhat more lenient criterion of 5.0 Å distance from the sulfur.

Results

Inhibition of p300 HAT Activity by CyPGs

In vitro p300 HAT assays using [acetyl-1-^{14}C] CoA and HeLa core histones with the recombinant p300 HAT domain that was preincubated with various concentrations (100 nM-5 μM) of PGs clearly indicated an interesting pattern. While PGD_2, PGE_2, PGK_2, PGB_2, and PGA_2 failed to inhibit the HAT activity of p300, Δ^{12}-PGJ_2 and PGJ_2 (Δ^{13}-PGJ_2) inhibited the activity of p300 significantly. The IC_{50} values with Δ^{12}-PGJ_2 and PGJ_2 were calculated to be ~750 nM and >2 μM, respectively (Figure 1). Furthermore, Δ^{12}-PGJ_2 and PGJ_2, being positional isomers, showed differences in their reactivities toward the inhibition of p300 activity. However, Δ^{12}-PGJ_2 failed to inhibit recombinant PCAF activity even at 5 μM (data not shown). PGD_2, PGE_2, PGK_2, and 9,10-dihydro-15-deoxy-$\Delta^{12,14}$-PGJ_2 lack an unsaturation at carbon-9 and did not exhibit any inhibitory properties. It should also be noted that PGD_2, the precursor for CyPGs of the J_2 class, did not affect HAT activity, while the dehydration product (Δ^{12}-PGJ_2) was effective toward HAT p300 suggesting that metabolism to CyPGs is essential for activity.

The ability of these PGs to inhibit cellular p300 HAT activity was tested in HepG2, a human hepatocarcinoma cell line, where histones (H3 and H4) are known to be hyper acetylated.[36,40] As a preliminary screen, HepG2 cells were treated with 10 μM of each of the PGs. No significant toxicities were observed (Supporting Information, Figure S1). As shown in Figure 2, treatment with Δ^{12}-PGJ_2 and PGJ_2 showed significant reduction in the histone H3 acetylation level. (Figure 2A; lanes 2 and 3). PGA_2 showed a nonsignificant decrease (Figure 2A; lane 10). However, PGE_2, PGB_2, PGK_2, 9,10-dihydro-15-deoxy-$\Delta^{12,14}$-PGJ_2, PGD_2, and 13,14-dihydro-PGD_2 were ineffective at inhibiting acetylation in these cells (Figure 2A; lanes 4–9). On the basis of these results, it became clear that Δ^{12}-PGJ_2 appeared to be a potent inhibitor of p300. Thus, we used Δ^{12}-PGJ_2 as a lead compound for further studies. Treatment of HepG2 cells with increasing concentrations (0.5-10 μM) of Δ^{12}-PGJ_2 showed a dose-dependent inhibition of histone H3 K9/K14 acetylation, with more than 90% inhibition at 10 μM of Δ^{12}-PGJ_2 compared to the DMSO control (Figure 3A; compare lane 1 vs lane 3). The IC_{50} was calculated to be ~5 μM.

To address if endogenously produced CyPGs were capable of inhibiting HAT activity, we used a murine macrophage (RAW264.7) cell model that has been shown by our laboratory to produce high levels of CyPG when cultured in the presence of a fully expressed selenoproteome.[3,41] As shown in Figure 3C, treatment of such cells with either indomethacin (10 μM) or HQL-79 (25 μM), which inhibit COX-1/2 and H-PGDS, respectively, clearly demonstrated an increased acetylation of histone H3K9/K14 compared

to that of the DMSO control. Treatment of RAW264.7 cells with indomethacin or HQL-79 did not show any effect on HDAC-1 expression (data not shown). These results provide sufficient proof-of-concept that endogenous CyPG have the ability to modulate HAT activity.

Δ^{12}-PGJ$_2$ Inhibits p300 by Michael Addition

On the basis of the differences in the ability of Δ^{12}-PGJ$_2$ and 9,10-dihydro-15-deoxy-$\Delta^{12,14}$-PGJ$_2$ to inhibit p300 activity, and the fact that the substrate-binding site of p300 contains a Cys residue (aa 1438), we speculated that p300 perhaps covalently interacted with Δ^{12}-PGJ$_2$. To examine the interaction of Δ^{12}-PGJ$_2$, biotinylated Δ^{12}-PGJ$_2$ and 9,10-dihydro-15-deoxy-$\Delta^{12,14}$-PGJ$_2$ were used. 9,10-Dihydro-15-deoxy-$\Delta^{12,14}$-PGJ$_2$ was mainly used as a control. The biotinylated compounds were incubated with the recombinant p300 HAT domain for 3 h, and the binding of biotinylated derivatives of Δ^{12}-PGJ$_2$ or 9,10-dihydro-15-deoxy-$\Delta^{12,14}$-PGJ$_2$ to p300 was analyzed by SDS–PAGE under denaturing conditions followed by Western blotting with neutravidin-HRP and GST. Figure 4A clearly indicates the binding of Δ^{12}-PGJ$_2$ to p300; while 9,10-dihydro-derivative was ineffective. To further address if this interaction was intact even in the presence of other proteins, nuclear extracts from U937 human monocytic cells were mixed with recombinant p300 to which biotinylated CyPGs were added. These samples were subjected to pull-down with neutravidin–agarose beads overnight. The binding of p300 to biotinylated Δ^{12}-PGJ$_2$ or biotinylated 9,10-dihydro-15-deoxy-$\Delta^{12,14}$-PGJ$_2$ was analyzed by gel electrophoresis and immunoblotting with anti-GST antibody (Figure 4A), followed by probing the same membrane with the neutravidin–HRP conjugate (Figure 4A). The results in Figure 4A clearly demonstrate that the presence or absence of nuclear proteins did not affect the interaction of biotinylated Δ^{12}-PGJ$_2$ with p300, while biotinylated 9,10-dihydro-15-deoxy-$\Delta^{12,14}$-PGJ$_2$ did not interact with p300. Furthermore, in the above *in vitro* reaction, a peptide containing the reactive Cys[1438] was coincubated with the p300 HAT domain and Δ^{12}-PGJ$_2$ at 1:1 and 1:2 molar ratios (p300/peptide) for 3 h followed by immunoblotting with the neutravidin-HRP conjugate to examine the biotinylation of p300. As expected, the peptide inhibited the interaction of Δ^{12}-PGJ$_2$ with p300 at both 1:1 and 1:2 molar ratios (Figure 4B). Taken together, these results strongly support the ability of Δ^{12}-PGJ$_2$ to interact with p300 by forming a covalent adduct.

Δ^{12}-PGJ$_2$ Interacts Covalently with Cys[1438] in p300 HAT

Given the presence of Cys[1438] in the active site of p300, we examined its role as a nucleophilic acceptor for the binding of Δ^{12}-PGJ$_2$ in the following studies. First, the p300 peptide (GHIWA**C**PPSEG) or mutant peptide lacking Cys (GHI-WA**A**PPSEG) corresponding to amino acids 1433–1443 in p300 was incubated for 3 h with molar equivalents of Δ^{12}-PGJ$_2$, and the complex was analyzed by LC-MS as well as by direct infusion. As shown in Figure 5(A,B), the native peptide and the peptide-Δ^{12}-PGJ$_2$ adduct could be separated by LC. An increase in the *m/z* of molecular ion of the peptide from 1153.2 to 1487.0 clearly indicated that the peptide interacted covalently with Δ^{12}-PGJ$_2$ (Figure 5C,D). Second, mutagenesis of Cys[1438] to Ala in the substrate binding site of the p300 HAT domain followed by *in vitro* binding studies with Δ^{12}-PGJ$_2$-biotinamide clearly indicated that Cys[1438] was indispensible for the covalent interaction of Δ^{12}-PGJ$_2$ with p300 (Figure 6A,B). Incubation of the mutant peptide with the p300 HAT domain and Δ^{12}-PGJ$_2$ demonstrated a clear lack of competition with p300 for Δ^{12}-PGJ$_2$ (Figure 5B). In addition, incubation of the mutant peptide with Δ^{12}-PGJ$_2$ did not lead to a corresponding increase in the molecular mass of the peptide.

To probe this interaction further, we utilized a molecular modeling approach using the crystal structure of the HAT domain of p300 liganded to a synthetic inhibitor, lysyl-CoA, reported recently.[38] In order to gauge the propensity for PGs to bind to p300-HAT via

precovalent conformations suitable for covalent reaction with binding site nucleophiles, we examined the model generated from the crystal structure of p300-HAT for solvent-exposed Cys residues within close proximity of the cocrystallized CoA ligand. Using this structure, molecular modeling studies with different CyPGs were performed. As shown in Figure 7, all of the PGs tested were seen to bind to p300 HAT. Of these, Δ^{12}-PGJ$_2$ was found to have the strongest affinity for this putative covalent binding mode (Surflex score = 7.86), followed by 9,10-dihydro-15-deoxy-$\Delta^{12,14}$-PGJ$_2$ (7.18), PGK$_2$ (6.49), and 15d-PGJ$_2$ (6.07). Further analysis of the interaction between Δ^{12}-PGJ$_2$ and Cys^{1438} showed that the electrophilic carbon-9 was positioned within 4 Å of the nucleophilic Cys-S$^-$ to facilitate the formation of an adduct. 9,10-Dihydro-15-deoxy-$\Delta^{12,14}$-PGJ$_2$ also snuggly fit into the substrate binding site but was not capable of interacting with Cys^{1438} due to the lack of an electrophilic carbon as shown in Figure 7A. Interestingly, the two hydrophobic tails of Δ^{12}-PGJ$_2$ were positioned around the antiparallel β-sheets in p300 such that the electrophilic center at carbon-9 in the cyclopentenone was placed in the vicinity of Cys1438 (Figure 7B–D). However, in the case of PGA$_2$, PGK$_2$, and PGB$_2$, which were ineffective in inhibiting H3 acetylation, the positioning of the α,β-unsaturated reactive center was farther away from the Cys^{1438}, thus making them less likely to interact with the nucleophilic Cys-S$^-$ in the substrate binding site. Taken together, these studies further provide support to the premise that Δ^{12}-PGJ$_2$ covalently interacts with p300 via the Cys^{1438} in the substrate-binding pocket of p300.

Δ^{12}-PGJ$_2$ Inhibits the Acetylation of HIV-1 Tat Protein by p300 HAT

It has been previously shown that the HIV Tat protein, which serves as a substrate for p300, is acetylated at K50 and K51 and that this acetylation is important for its activity.[42] To examine if Δ^{12}-PGJ$_2$-dependent inhibition of p300 HAT activity had any effect on the acetylation of Tat, the p300 HAT domain was incubated in the presence or absence of Δ^{12}-PGJ$_2$ (1:3) for 3 h at room temperature. Recombinant Tat protein (His-tagged) and [acetyl-1-^{14}C] CoA were added to the p300 HAT-Δ^{12}-PGJ$_2$ complex, and the reaction mixture was incubated for an additional 1 h at room temperature. rTat was subjected to pull-down with HisPur resin and washed with PBS, and the beads were boiled with SDS-PAGE gel loading buffer. Radioactivity in the supernatant was counted by scintillation counting. As expected, rTat was acetylated by the p300 HAT domain that was not preincubated with Δ^{12}-PGJ$_2$ (Figure 8A). However, the p300 HAT domain that was alkylated (carbonylated) by Δ^{12}-PGJ$_2$ exhibited significantly low acetylation activity toward rTat. It was observed that the acetylation of rTat by p300 was inhibited upon incubation of the HAT domain with Δ^{12}-PGJ$_2$ (Figure 8A). Furthermore, we extended the analysis to examine the effect of Δ^{12}-PGJ$_2$ treatment of U1/HIV cells (human monocytic cells chronically infected with HIV-1) that were previously stimulated with PMA to activate the expression of the integrated provirus. Treatment of such cells with Δ^{12}-PGJ$_2$ (2 μM) for 24 and 48 h clearly showed differences in the levels of acetylation of H3 (at K9 and K14), as a function of time (Figure 8B). While the decrease in Ac-H3 on day 1 was not substantial (Figure 8B; compare lane 1 vs 2), the decrease in Ac-H3 on day 2 post treatment was greatly decreased (Figure 8B; compare lane 3 vs 4). Treatment with 2 μM of Δ^{12}-PGJ$_2$ for 2 days did not cause any toxicity in these cells (Supporting Information, Figure S2). Levels of p24, a component of the HIV virus capsid in the supernatant of these PMA-stimulated cells also showed a significant (~70%) decrease upon treatment with Δ^{12}-PGJ$_2$, particularly at day 2 post-treatment (Figure 8C). Taken together, these studies indicate that Δ^{12}-PGJ$_2$ is a potent inhibitor of p300-dependent acetylation of Tat as well as H3 in HIV-infected cells, which contributes, in part, to the reduction in HIV proviral expression.

Discussion

Many studies have documented an important role for CyPGs as key modulators of gene expression by their ability to modify proteins involved in signaling transduction cascades, chromatin dynamics, and transcription factors.[40] Such an interaction with proteins, mainly through Cys thiols, contributes to the pleiotropic effects of these reactive metabolites of PGD_2. Although beneficial effects of CyPGs are reported in experimental models of inflammation, CyPGs are also known to promote proliferation and angiogenesis.[43,44] Thus, given the ability of these molecules to act in a context-specific, cell-specific, and concentration-dependent manner, it is very likely that CyPGs may impact many vital cellular processes that continue to unfold. In continuation of our quest into the characterization of the CyPG interactome, we report here, for the first time, that Δ^{12}-PGJ_2, a metabolic end product of arachidonic acid-derived PGD_2, inhibits the enzymatic activity of p300 HAT. Site-directed mutagenesis and peptide competition experiments further indicated that the inhibition of p300 HAT activity by Δ^{12}-PGJ_2 occurred via the alkylation of Cys[1438] in the substrate-binding site. This is in contrast to the role of 15d-PGJ_2, a dehydrated product of Δ^{12}-PGJ_2, which has been shown to inactivate HATs through their insolubilization in HepG2 cells; while Δ^{12}-PGJ_2 did not affect the stability of p300.[45] Furthermore, 15d-PGJ_2 also has been shown to inhibit mammalian class I HDACs by covalent binding to two conserved Cys.[46] Thus, given these effects of 15d-PGJ_2, we have excluded this molecule from the current studies.

Although the molecular basis of epigenetic regulation of gene expression is complex, there is now a clear understanding that HATs, such as p300 and its paralogue CREB-binding protein (CBP), modify the unstructured N-termini of histones (called "histone tails"), and are generally correlated with transcriptional competence and diverse biological processes. However, the ability of p300 to impact the function of many histone and nonhistone proteins by acetylation has further invigorated the search for specific inhibitors of this key transferase.[47] The "relaxed" substrate specificity of p300 is attributed due to the lack of a deep substrate-binding pocket that potentially prohibits the formation of a stable ternary complex between the enzyme and the two cosubstrates.[38] These studies reporting the ability of Δ^{12}-PGJ_2 to inhibit the activity of p300 by a unique mechanism involving the nucleophilic Cys in the substrate binding site opens a new area in the field of eicosanoid-dependent regulation of gene expression, particularly in inflammation and HIV biology.

The ability of CyPGs to interact with nucleophiles, particularly Cys thiols (thiolate anion), provides the basis for the biological effects. However, this depends largely on whether cells can produce such high amounts of free CyPGs in cells. One might speculate that localized concentrations of CyPGs in the high nanomolar range may be possible given the fact that COX isozymes, which are membrane bound, functionally couple with downstream PGDS isozymes, which are mostly cytosolic, to produce PGD_2 that undergoes nonenzymatic dehydration and isomerization to form PGJ_2, Δ^{12}-PGJ_2, and 15d-PGJ_2. In fact, recent reports from our laboratory have demonstrated the role of micronutrient selenium (Se), in the form of selenoproteins, to shunt pathways of arachidonic acid metabolism from PGE_2 to PGD_2 metabolites in macrophages.[3,41] Our macrophage model is capable of producing relatively high concentrations of Δ^{12}-PGJ_2. As a result, the production of high levels of extracellular Δ^{12}-PGJ_2 relative to its dehydration product, 15d-PGJ_2, was observed in macrophages supplemented with Se, which is not surprising given the thermodynamic constraints associated with the final dehydration of Δ^{12}-PGJ_2 to 15d-PGJ_2.[3,48] Studies with such Seenriched macrophages demonstrate the inhibition of acetylation of H3K9/14 by indomethacin and HQL-79, when compared to the vehicle control, suggesting the endogenous production of CyPG to inhibit HAT activity. Further studies to correlate the

effects of enhanced cellular production of CyPGs on acetylation of histone and nonhistone proteins are currently underway in our laboratory and will be reported in the near future.

Our results show an interesting structure–function correlation wherein Δ^{12}-PGJ$_2$ and its positional isomer, PGJ$_2$ (Δ^{13}-PGJ$_2$), differ in their ability to inhibit p300, with Δ^{12}-PGJ$_2$ being more reactive than Δ^{13}-PGJ$_2$. Comparing the two isomers, the presence of a conjugated diene structure following tautomeric rearrangement of electrons within the cyclopentenone ring possibly makes the carbon 9 more electrophilic; while in the case of PGJ$_2$, due to the presence of an unsaturation at carbon 13, a relatively less electrophilic nature of carbon 9 may help explain the differences in their inhibitory activities.[9] The differences in the reactivity of CyPGs isomers are reminiscent of their interaction with GSH as reported by Atsmon et al.[9] On the basis of the molecular modeling studies, all PGs tested, including 9,10-dihydro-15d-PGJ$_2$, seem to enter the substrate-binding site in p300, where the positioning of the electrophilic carbon 9 in the close vicinity of Cys[1438] appears to be critical for the inhibitory activity. Along the same lines, PGA$_2$ and PGB$_2$, although CyPGs, were ineffective as inhibitors of p300, possibly owing to the position of its electrophilic carbon. Similarly, PGK$_2$ that lacks an alkylidenecyclopentenone structure did not inhibit the enzyme even though the cyclopentanedione ring was likely to orient π orbitals favorably for S nucleophilic attack. This is in contrast to that in HDACs, where even an unrelated electrophile like 4-hydroxynonenal binds to the Cys residues.[46] Thus, it appears that binding and positioning of the electrophilic carbon 9 in CyPGs to the nucleophilic Cys[1438] determines the selectivity. Experiments showing the abrogation of interaction of p300 HAT domain with Δ^{12}-PGJ$_2$ upon incubation of p300 peptide containing Cys[1438] further suggest that accessibility of the Cys residue plays an equally important role, which is reminiscent of the interaction of CyPGs with specific Cys residues in thioredoxin, GSTP1-1, ubiquitin carboxyl-terminal hydrolase-1, and H-Ras.[18,19,49,50] Along these lines, we have previously described the ability of CyPGs to interact with Cys thiols in HIV-1 Tat, and here, we demonstrate that the consequence of inhibition of p300 has a major effect on the activation of Tat and HIV replication in general (Figure 8B,C), accompanied by a decrease in H3 acetylation levels.[14]

On the basis of the discussion above, it is clear that the mere presence of an α,β-unsaturated carbonyl structure is not sufficient to inhibit p300 activity. That said, natural products like curcumin, plumbagin, and garcinol, which also contain α,β-unsaturated carbonyl functionalities, inhibit p300 HAT activity through a different mechanism involving a weak hydrogen bonding with Lys[1358].[31–33,35,36] Furthermore, oxo-containing metabolites of lipid mediators, such as 17-oxo-RvD1, which are formed endogenously from docosahexaenoic acid, could also modulate HAT activity by forming Michael adducts.[51] Thus, it would be interesting to examine the ability of all these (natural) compounds to interact with Cys[1438] to better appreciate the stereoselectivity as well as define their role in modulating gene expression. Interestingly, our results are in agreement with those reported with plumbagin with regard to the increased specificity toward p300 rather than PCAF.[36] This is not surprising since the active site of PCAF lacks the presence of a nucleophilic residue in the form of a conserved Cys648 residue that is too far from the active site.[52]

In summary, we have identified an oxidized fatty acid metabolite as a p300 HAT inhibitor. Our data supports the selective inhibition of p300 HAT activity only by certain CyPGs, based on their ability to interact covalently with Cys[1438], a key residue that is pivotal for the binding of substrates, to form a Michael adduct. Although the observed IC$_{50}$ of Δ^{12}-PGJ$_2$ toward p300 is higher than the concentration of Δ^{12}-PGJ$_2$ produced in the macrophage model, the cellular data may not correlate entirely with the *in vitro* analysis due to many factors, such as the use of the p300 HAT domain in isolation that could alter the structure of this domain in the absence of other interaction partners, lowering the reactivity and

accessibility of the Cys thiol. Needless to say, these studies need to be evaluated in the light of tissue and cell-specific toxicity of CyPGs. Our studies demonstrating the targeting of p300 with Δ^{12}-PGJ$_2$ on the acetylation of Tat opens a new window of opportunity to regulate proviral transcriptional replication. Such studies are likely to further expand to examine the effect of inhibition of p300 by Δ^{12}-PGJ$_2$ on many other transcription factors to provide a better understanding of the role of this class of endogenous metabolites in areas such as resolution of inflammation, where CyPGs are already known to facilitate the process. Although preliminary studies on the inability of Δ^{12}-PGJ$_2$ to inhibit PCAF suggests some level of selectivity, further studies are required to examine the effect of these CyPGs on other classes of HAT enzymes, where a similar mechanism may be followed.[53,54]

Supplementary Material

Refer to Web version on PubMed Central for supplementary material.

Acknowledgments

References

1. Smith WL, DeWitt DL, Garavito RM. Cyclooxygenases: structural, cellular, and molecular biology. Annu Rev Biochem. 2000; 69:145–182. [PubMed: 10966456]

2. Fukushima M, Kato T, Narumiya S, Mizushima Y, Sasaki H, Terashima Y, Nishiyama Y, Santoro MG. Prostaglandin A and J: antitumor and antiviral prostaglandins. Adv Prostaglandins, Thromboxanes, Leukotrienes Res. 1989; 19:415–418.

3. Gandhi UH, Kaushal N, Ravindra KC, Hegde S, Nelson SM, Narayan V, Vunta H, Paulson RF, Prabhu KS. Selenoprotein-dependent up-regulation of hematopoietic prostaglandin D2 synthase in macrophages is mediated through the activation of peroxisome proliferator-activated receptor (PPAR) {gamma}. J Biol Chem. 2011; 286:27471–27482. [PubMed: 21669866]

4. Itoh K, Mochizuki M, Ishii Y, Ishii T, Shibata T, Kawamoto Y, Kelly V, Sekizawa K, Uchida K, Yamamoto M. Transcription factor Nrf2 regulates inflammation by mediating the effect of 15-deoxy-Delta(12,14)-prostaglandin j(2). Mol Cell Biol. 2004; 24:36–45. [PubMed: 14673141]

5. Kliewer SA, Lenhard JM, Willson TM, Patel I, Morris DC, Lehmann JM. A prostaglandin J2 metabolite binds peroxisome proliferator-activated receptor gamma and promotes adipocyte differentiation. Cell. 1995; 83:813–819. [PubMed: 8521498]

6. Lee TS, Tsai HL, Chau LY. Induction of heme oxygenase-1 expression in murine macrophages is essential for the anti-inflammatory effect of low dose 15-deoxy-Delta 12,14-prostaglandin J2. J Biol Chem. 2003; 278:19325–19330. [PubMed: 12642589]

7. Rossi A, Kapahi P, Natoli G, Takahashi T, Chen Y, Karin M, Santoro MG. Anti-inflammatory cyclopentenone prostaglandins are direct inhibitors of IkappaB kinase. Nature. 2000; 403:103–108. [PubMed: 10638762]

8. Straus DS, Glass CK. Cyclopentenone prostaglandins: new insights on biological activities and cellular targets. Med Res Rev. 2001; 21:185–210. [PubMed: 11301410]

9. Atsmon J, Sweetman BJ, Baertschi SW, Harris TM, Roberts LJ II. Formation of thiol conjugates of 9-deoxy-delta 9,delta 12(E)-prostaglandin D2 and delta 12(E)-prostaglandin D2. Biochemistry. 1990; 29:3760–3765. [PubMed: 2340271]

10. Shiraki T, Kamiya N, Shiki S, Kodama TS, Kakizuka A, Jingami H. Alpha,beta-unsaturated ketone is a core moiety of natural ligands for covalent binding to peroxisome proliferator-activated receptor gamma. J Biol Chem. 2005; 280:14145–14153. [PubMed: 15695504]
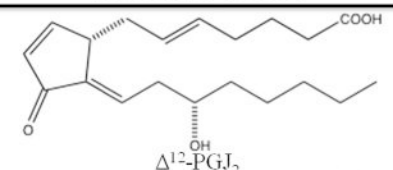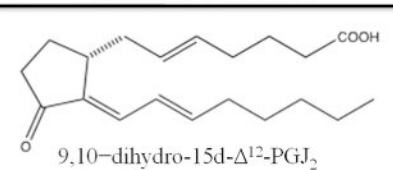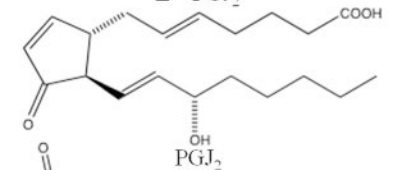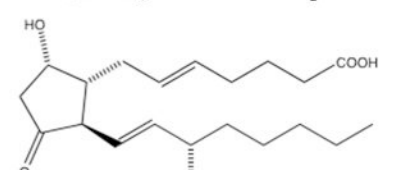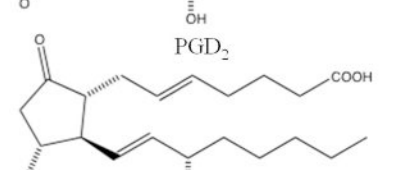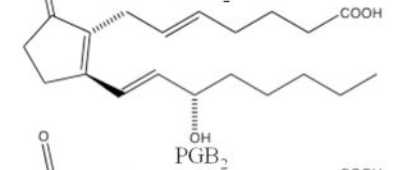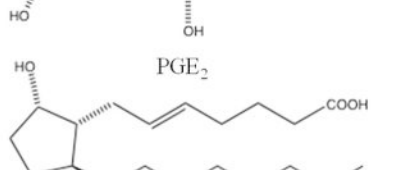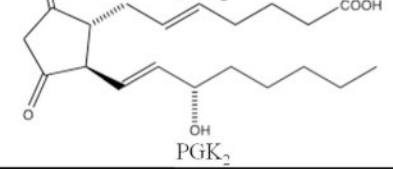
11. Stamatakis K, Perez-Sala D. Prostanoids with cyclopentenone structure as tools for the characterization of electrophilic lipid-protein interactomes. Ann NY Acad Sci. 2006; 1091:548–570. [PubMed: 17341644]

12. Suzuki M, Mori M, Niwa T, Hirata R, Furuta K, Ishikawa T, Noyori R. Chemical implications for antitumor and antiviral prostaglandins: reaction of Δ7-prostaglandin A1 and prostaglandin A1methyl esters with thiols. J Am Chem Soc. 1997; 119:2376–2385.

13. Gayarre J, Stamatakis K, Renedo M, Perez-Sala D. Differential selectivity of protein modification by the cyclopentenone prostaglandins PGA1 and 15-deoxy-Delta12,14-PGJ2: role of glutathione. FEBS Lett. 2005; 579:5803–5808. [PubMed: 16223487]

14. Kalantari P, Narayan V, Henderson AJ, Prabhu KS. 15-Deoxy-Delta12,14-prostaglandin J2 inhibits HIV-1 transactivating protein, Tat, through covalent modification. FASEB J. 2009; 23:2366–2373. [PubMed: 19299483]

15. Kim DH, Kim EH, Na HK, Sun Y, Surh YJ. 15-Deoxy-Delta(12,14)-prostaglandin J(2) stabilizes, but functionally inactivates p53 by binding to the cysteine 277 residue. Oncogene. 2010; 29:2560–2576. [PubMed: 20208557]

16. Kobayashi M, Li L, Iwamoto N, Nakajima-Takagi Y, Kaneko H, Nakayama Y, Eguchi M, Wada Y, Kumagai Y, Yamamoto M. The antioxidant defense system Keap1-Nrf2 comprises a multiple sensing mechanism for responding to a wide range of chemical compounds. Mol Cell Biol. 2009; 29:493–502. [PubMed: 19001094]

17. Noyori R, Suzuki M. Organic synthesis of prostaglandins: advancing biology. Sci. 1993; 259:44–45.

18. Oliva JL, Perez-Sala D, Castrillo A, Martinez N, Canada FJ, Bosca L, Rojas JM. The cyclopentenone 15-deoxy-delta 12,14-prostaglandin J2 binds to and activates H-Ras. Proc Natl Acad Sci USA. 2003; 100:4772–4777. [PubMed: 12684535]

19. Shibata T, Yamada T, Ishii T, Kumazawa S, Nakamura H, Masutani H, Yodoi J, Uchida K. Thioredoxin as a molecular target of cyclopentenone prostaglandins. J Biol Chem. 2003; 278:26046–26054. [PubMed: 12709421]

20. Cernuda-Morollon E, Pineda-Molina E, Canada FJ, Perez-Sala D. 15-Deoxy-Delta 12,14-prostaglandin J2 inhibition of NF-kappaB-DNA binding through covalent modification of the p50 subunit. J Biol Chem. 2001; 276:35530–35536. [PubMed: 11466314]

21. Batta K, Das C, Gadad S, Shandilya J, Kundu TK. Reversible acetylation of non histone proteins: role in cellular function and disease. Subcell Biochem. 2007; 41:193–212. [PubMed: 17484129]

22. van Attikum H, Gasser SM. The histone code at DNA breaks: a guide to repair? Nat Rev Mol Cell Biol. 2005; 6:757–765. [PubMed: 16167054]

23. Wei Y, Yu L, Bowen J, Gorovsky MA, Allis CD. Phosphorylation of histone H3 is required for proper chromosome condensation and segregation. Cell. 1999; 97:99–109. [PubMed: 10199406]

24. Grant PA, Berger SL. Histone acetyltransferase complexes. Semin Cell Dev Biol. 1999; 10:169–177. [PubMed: 10441070]

25. Roth SY, Denu JM, Allis CD. Histone acetyltransferases. Annu Rev Biochem. 2001; 70:81–120. [PubMed: 11395403]

26. Barnes PJ, Adcock IM, Ito K. Histone acetylation and deacetylation: importance in inflammatory lung diseases. Eur Respir J. 2005; 25:552–563. [PubMed: 15738302]

27. Iyer NG, Ozdag H, Caldas C. p300/CBP and cancer. Oncogene. 2004; 23:4225–4231. [PubMed: 15156177]

28. McKinsey TA, Olson EN. Cardiac histone acetylation: therapeutic opportunities abound. Trends Genet. 2004; 20:206–213. [PubMed: 15041175]

29. Pumfery A, Deng L, Maddukuri A, de la Fuente C, Li H, Wade JD, Lambert P, Kumar A, Kashanchi F. Chromatin remodeling and modification during HIV-1 Tat-activated transcription. Curr HIV Res. 2003; 1:343–362. [PubMed: 15046258]

30. Sterner DE, Berger SL. Acetylation of histones and transcription-related factors. Microbiol Mol Biol Rev. 2000; 64:435–459. [PubMed: 10839822]

31. Balasubramanyam K, Altaf M, Varier RA, Swaminathan V, Ravindran A, Sadhale PP, Kundu TK. Polyisoprenylated benzophenone, garcinol, a natural histone acetyltransferase inhibitor, represses

chromatin transcription and alters global gene expression. J Biol Chem. 2004; 279:33716–33726. [PubMed: 15155757]

32. Balasubramanyam K, Swaminathan V, Ranganathan A, Kundu TK. Small molecule modulators of histone acetyltransferase p300. J Biol Chem. 2003; 278:19134–19140. [PubMed: 12624111]

33. Balasubramanyam K, Varier RA, Altaf M, Swaminathan V, Siddappa NB, Ranga U, Kundu TK. Curcumin, a novel p300/CREB-binding protein-specific inhibitor of acetyltransferase, represses the acetylation of histone/nonhistone proteins and histone acetyltransferase-dependent chromatin transcription. J Biol Chem. 2004; 279:51163–51171. [PubMed: 15383533]

34. Lau OD, Kundu TK, Soccio RE, Ait-Si-Ali S, Khalil EM, Vassilev A, Wolffe AP, Nakatani Y, Roeder RG, Cole PA. HATs off: selective synthetic inhibitors of the histone acetyltransferases p300 and PCAF. Mol Cell. 2000; 5:589–595. [PubMed: 10882143]

35. Mantelingu K, Reddy BA, Swaminathan V, Kishore AH, Siddappa NB, Kumar GV, Nagashankar G, Natesh N, Roy S, Sadhale PP, Ranga U, Narayana C, Kundu TK. Specific inhibition of p300-HAT alters global gene expression and represses HIV replication. Chem Biol. 2007; 14:645–657. [PubMed: 17584612]

36. Ravindra KC, Selvi BR, Arif M, Reddy BA, Thanuja GR, Agrawal S, Pradhan SK, Nagashayana N, Dasgupta D, Kundu TK. Inhibition of lysine acetyltransferase KAT3B/p300 activity by a naturally occurring hydroxynaphthoquinone, plumbagin. J Biol Chem. 2009; 284:24453–24464. [PubMed: 19570987]

37. Bowers EM, Yan G, Mukherjee C, Orry A, Wang L, Holbert MA, Crump NT, Hazzalin CA, Liszczak G, Yuan H, Larocca C, Saldanha SA, Abagyan R, Sun Y, Meyers DJ, Marmorstein R, Mahadevan LC, Alani RM, Cole PA. Virtual ligand screening of the p300/CBP histone acetyltransferase: identification of a selective small molecule inhibitor. Chem Biol. 2010; 17:471–482. [PubMed: 20534345]

38. Liu X, Wang L, Zhao K, Thompson PR, Hwang Y, Marmorstein R, Cole PA. The structural basis of protein acetylation by the p300/CBP transcriptional coactivator. Nature. 2008; 451:846–850. [PubMed: 18273021]

39. Kundu TK, Palhan VB, Wang Z, An W, Cole PA, Roeder RG. Activator-dependent transcription from chromatin in vitro involving targeted histone acetylation by p300. Mol Cell. 2000; 6:551–561. [PubMed: 11030335]

40. Bai X, Wu L, Liang T, Liu Z, Li J, Li D, Xie H, Yin S, Yu J, Lin Q, Zheng S. Overexpression of myocyte enhancer factor 2 and histone hyperacetylation in hepatocellular carcinoma. J Cancer Res Clin Oncol. 2008; 134:83–91. [PubMed: 17611778]

41. Vunta H, Davis F, Palempalli UD, Bhat D, Arner RJ, Thompson JT, Peterson DG, Reddy CC, Prabhu KS. The anti-inflammatory effects of selenium are mediated through 15-deoxy-Delta12,14-prostaglandin J2 in macrophages. J Biol Chem. 2007; 282:17964–17973. [PubMed: 17439952]

42. Ott M, Schnolzer M, Garnica J, Fischle W, Emiliani S, Rackwitz HR, Verdin E. Acetylation of the HIV-1 Tat protein by p300 is important for its transcriptional activity. Curr Biol. 1999; 9:1489–1492. [PubMed: 10607594]

43. Millan O, Rico D, Peinado H, Zarich N, Stamatakis K, Perez-Sala D, Rojas JM, Cano A, Bosca L. Potentiation of tumor formation by topical administration of 15-deoxy-delta12,14-prostaglandin J2 in a model of skin carcinogenesis. Carcinogenesis. 2006; 27:328–336. [PubMed: 16113051]

44. Rajakariar R, Hilliard M, Lawrence T, Trivedi S, Colville-Nash P, Bellingan G, Fitzgerald D, Yaqoob MM, Gilroy DW. Hematopoietic prostaglandin D2 synthase controls the onset and resolution of acute inflammation through PGD2 and 15-deoxyDelta12 14 PGJ2. Proc Natl Acad Sci USA. 2007; 104:20979–20984. [PubMed: 18077391]

45. Hironaka A, Morisugi T, Kawakami T, Miyagi I, Tanaka Y. 15-Deoxy-Delta(12,14)-prostaglandin J(2) impairs the functions of histone acetyltransferases through their insolubilization in cells. Biochem Biophys Res Commun. 2009; 390:290–294. [PubMed: 19799872]

46. Doyle K, Fitzpatrick FA. Redox signaling, alkylation (carbonylation) of conserved cysteines inactivates class I histone deacetylases 1, 2, and 3 and antagonizes their transcriptional repressor function. J Biol Chem. 2010; 285:17417–17424. [PubMed: 20385560]

47. Wang L, Tang Y, Cole PA, Marmorstein R. Structure and chemistry of the p300/CBP and Rtt109 histone acetyltransferases: implications for histone acetyltransferase evolution and function. Curr Opin Struct Biol. 2008; 18:741–747. [PubMed: 18845255]

48. Maxey KM, Hessler E, MacDonald J, Hitchingham L. The nature and composition of 15-deoxy-Delta(12,14)PGJ(2). Prostaglandins Other Lipid Mediators. 2000; 62:15–21. [PubMed: 10936412]

49. Koharudin LM, Liu H, Di Maio R, Kodali RB, Graham SH, Gronenborn AM. Cyclopentenone prostaglandin-induced unfolding and aggregation of the Parkinson disease-associated UCH-L1. Proc Natl Acad Sci USA. 2010; 107:6835–6840. [PubMed: 20231490]

50. Sanchez-Gomez FJ, Diez-Dacal B, Pajares MA, Llorca O, Perez-Sala D. Cyclopentenone prostaglandins with dienone structure promote cross-linking of the chemoresistance-inducing enzyme glutathione transferase P1–1. Mol Pharmacol. 2010; 78:723–733. [PubMed: 20631055]

51. Sun YP, Oh SF, Uddin J, Yang R, Gotlinger K, Campbell E, Colgan SP, Petasis NA, Serhan CN. Resolvin D1 and its aspirin-triggered 17R epimer. Stereochemical assignments, anti-inflammatory properties, and enzymatic inactivation. J Biol Chem. 2007; 282:9323–9334. [PubMed: 17244615]

52. Clements A, Rojas JR, Trievel RC, Wang L, Berger SL, Marmorstein R. Crystal structure of the histone acetyltransferase domain of the human PCAF transcriptional regulator bound to coenzyme A. EMBO J. 1999; 18:3521–3532. [PubMed: 10393169]

53. Biel M, Kretsovali A, Karatzali E, Papamatheakis J, Giannis A. Design, synthesis, and biological evaluation of a small-molecule inhibitor of the histone acetyltransferase Gcn5. Angew Chem, Int Ed. 2004; 43:3974–3976.

54. Stimson L, Rowlands MG, Newbatt YM, Smith NF, Raynaud FI, Rogers P, Bavetsias V, Gorsuch S, Jarman M, Bannister A, Kouzarides T, McDonald E, Workman P, Aherne GW. Isothiazolones as inhibitors of PCAF and p300 histone acetyltransferase activity. Mol Cancer Ther. 2005; 4:1521–1532. [PubMed: 16227401]

Abbreviations

|	
HAT	histone acetyltransferase
PG	prostaglandin
PGD$_2$	prostaglandin D$_2$
Δ^{12}-PGJ$_2$	Δ^{12}-prostaglandin J$_2$
15d-PGJ$_2$	15-deoxy-$\Delta^{12,14}$-PGJ$_2$
CyPGs	cyclopentenone prostaglandins
CoA	coenzyme A
Se	selenium

Figure 1.
Structure of PGs along with their inhibitory activity toward p300. Each compound was tested for the inhibitory activity of p300 from 0.1 to 5 μM in *in vitro* assays, and IC$_{50}$ values were calculated. The average of three independent assays is shown. NA, no activity.
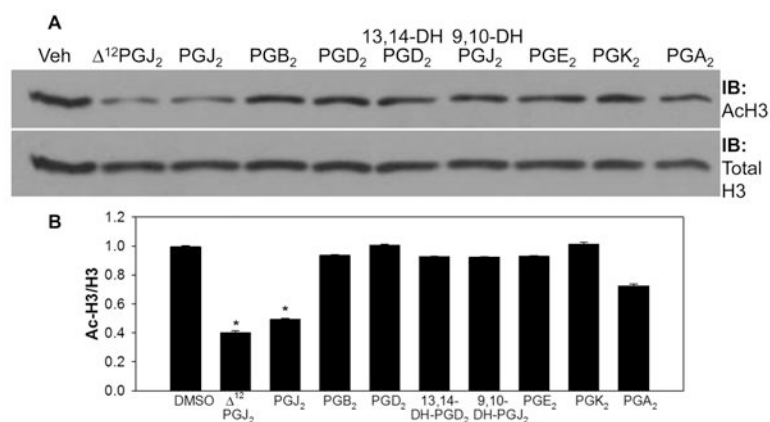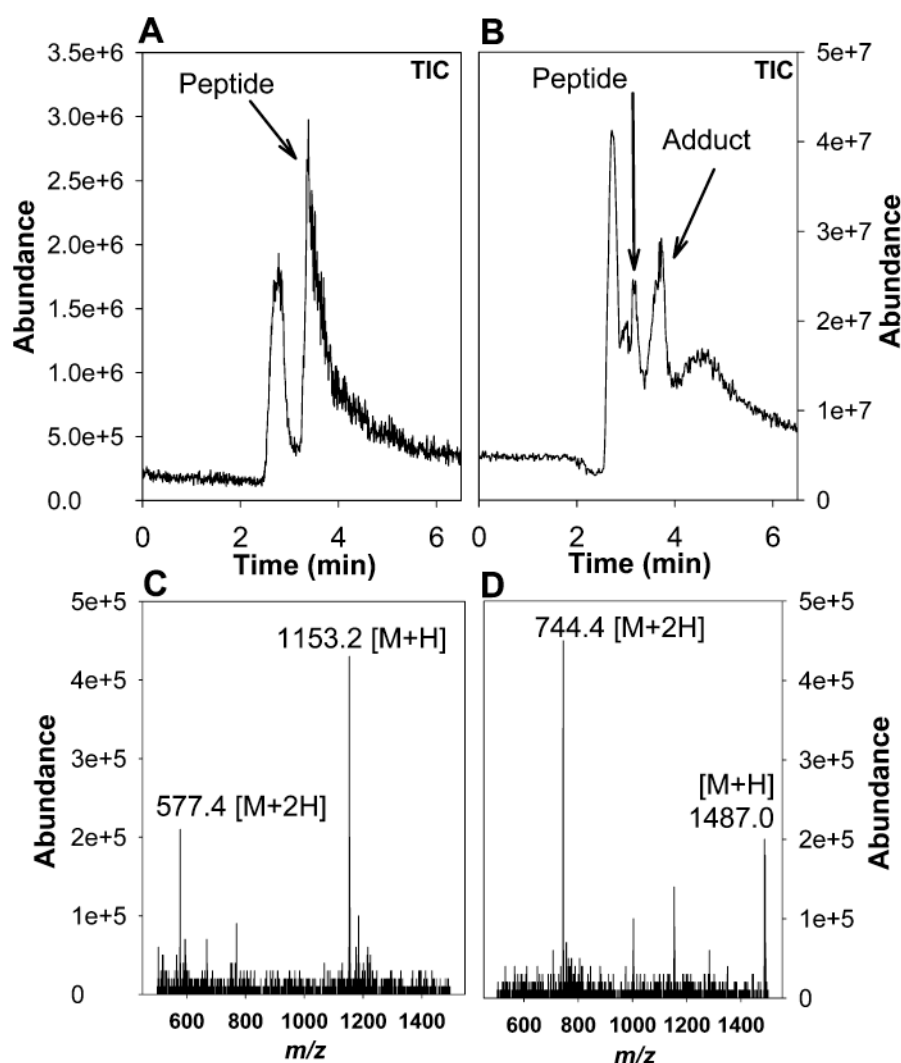
Figure 2.
Inhibition of H3 acetylation by PGs in HepG2 cells. (A) HepG2 cells were treated as indicated for 24 h; histones were isolated from DMSO treated cells (lane 1); PGs-treated cells at 10 μM concentration (lanes 2–10). The histone acetylation was analyzed by immunoblotting using acetylated H3 antibody and histone H3 as a loading control. (B) Densitometric analysis of total H3 versus acetylated H3. Mean ± SEM of three independent assays shown. *, $p < 0.00005$. 13,14-DH-PGD$_2$ and 9,10-DH-PGJ$_2$ represent 13,14-dihydro-15-keto-PGD$_2$ and 9,10-dihydro-15d-PGJ$_2$, respectively.
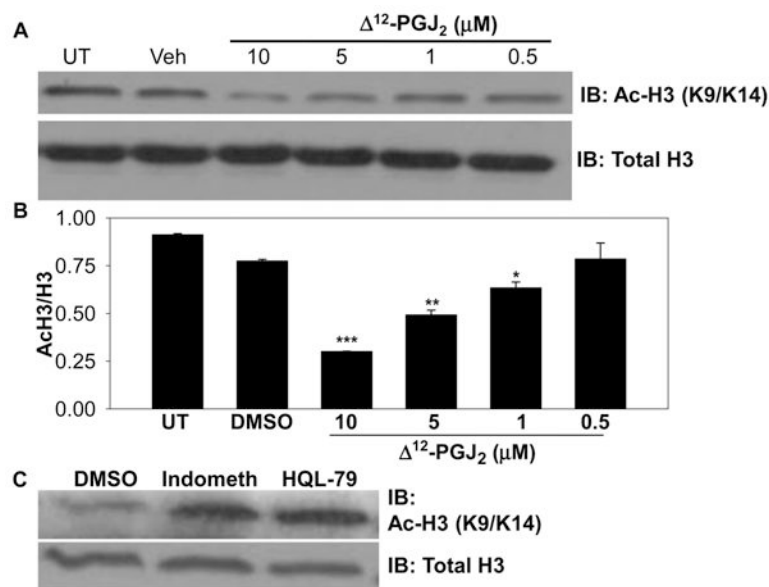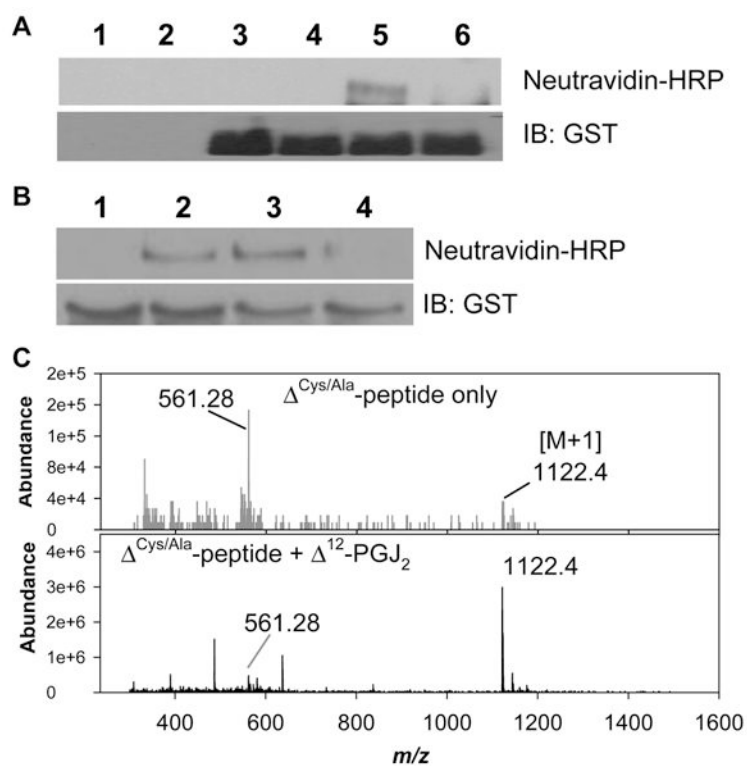
Figure 3.
Δ^{12}-PGJ$_2$ inhibits p300 acetylation of H3 in HepG2 and RAW264.7 cells. (A) HepG2 cells were treated with various concentrations of Δ^{12}-PGJ$_2$ for 24 h and histones were isolated from untreated cells (lane 1), DMSO treated cells (lane 2), Δ^{12}-PGJ$_2$-treated cells at 10 μM (lane 3), 5 μM (lane 4), 1 μM (lane 5), and 500 nM (lane 6). The histone acetylation was probed by immunoblotting using acetylated H3 antibody and histone H3 as a loading control. (B) Densitometry analysis of total H3 versus acetylated H3. Mean $\pm$ SEM values of three independent experiments are shown. *, $p < 0.05$; **, $p < 0.005$; ***, $p < 0.0005$. (C) RAW264.7 cells cultured in DMEM containing 250 nM sodium selenite was treated with DMSO, indomethacin (10 μM), or HQL-79 (25 μM) for 3 days following a 2 h LPS (50 ng/mL) exposure. Histones were isolated and acetylation of H3 at K9 and K14 was examined by immunoblotting. Representative of $n = 3$ is shown.
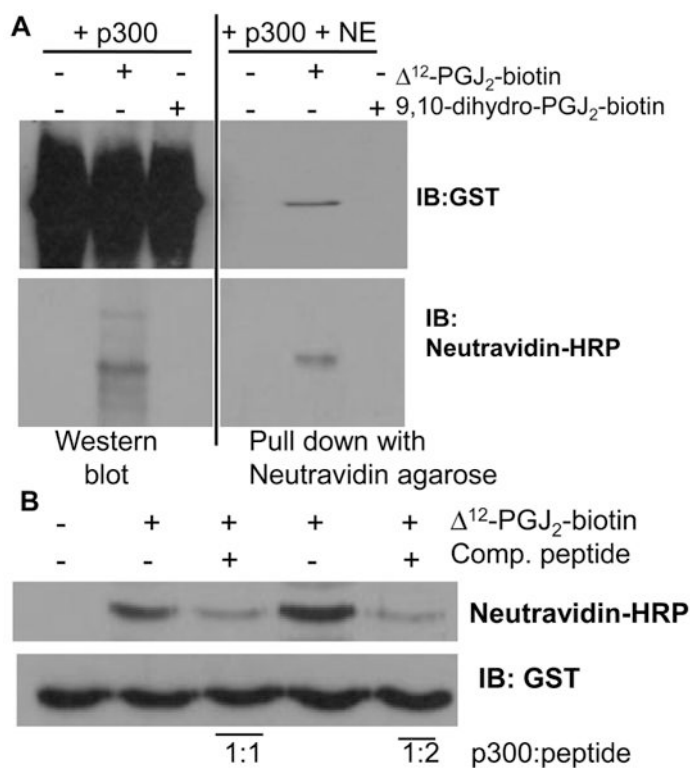
Figure 4.
Δ^{12}-PGJ$_2$ forms a covalent adduct with p300. (A) Left panel (Western blot): p300-GST was incubated with and without biotinylated PGs in an *in vitro* reaction. The reactions were analyzed by immunoblotting. Right panel (pull-down with neutravidin agarose): p300-GST was mixed with nuclear extracts (NE) from U937 monocytic cells and reacted with or without biotinylated PGs. These samples were subjected to pull-down with neutravidin–agarose beads and analyzed by immunoblotting. Representative of *n* = 2 shown. (B) Peptide competition assay. p300 only (lane 1), p300 and biotinylated Δ^{12}-PGJ$_2$ (lane 2), p300, biotinylated Δ^{12}-PGJ$_2$ and peptide (1:1 = p300: peptide; lane 3), p300 and biotinylated Δ^{12}-PGJ$_2$ (lane 4), p300, biotinylated Δ^{12}-PGJ$_2$ and peptide (1:2 = p300/peptide; lane 5). As a loading control, the blots were probed with GST. Representative of *n* = 2 is shown.
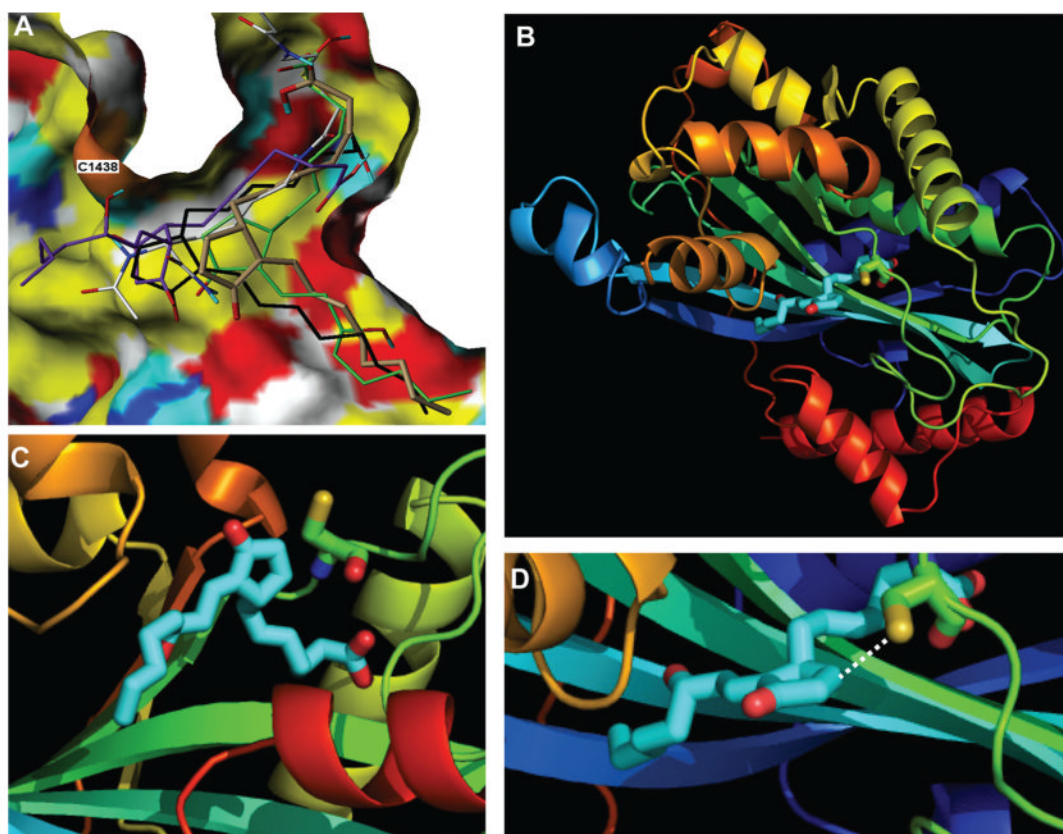
Figure 5.
LC-MS analysis of p300 peptide conjugated with Δ^{12}-PGJ$_2$. The peptides (0.3 μM) and Δ^{12}-PGJ$_2$ (0.3 μM) were incubated for 3 h in HAT assay buffer, in a reaction volume of 30 μL. The reactions were analyzed by LC-MS/MS as described in the Experimental Procedures section. The solvent system used was methanol/H$_2$O/acetic acid (70:30:0.1) at a flow rate 0.15 mL/min. Panels A and B represent p300 peptide only and p300 peptide incubated with Δ^{12}-PGJ$_2$, respectively. Panels C and D represent MS of the "peptide peak" and "adduct peak" from the TIC in panels A and B, respectively.
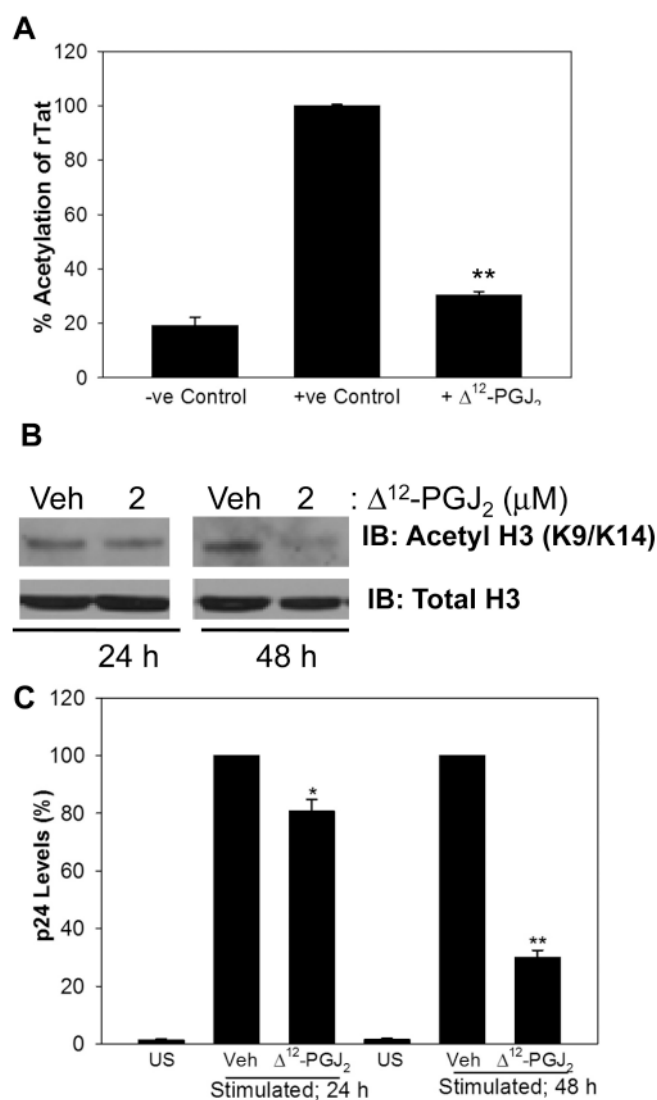
Figure 6.
Site-directed mutagenesis of p300 HAT domain. (A) Interaction of p300C1438A protein with Δ^{12}-PGJ$_2$. p300 wild type or C1438A mutant proteins were incubated with Δ^{12}-PGJ$_2$ biotinamide followed by SDS–PAGE analysis and Western blotting with neutravidin-HRP or GST. Lanes 1–6 represent, buffer alone, Δ^{12}-PGJ$_2$ biotinamide alone, native p300 only, p300-C1438A alone, native p300 + Δ^{12}-PGJ$_2$ biotinamide, and p300 C1438A + Δ^{12}-PGJ$_2$ biotinamide, respectively. (B) Peptide competition assay. In the above reaction, wild type or mutant peptides were included followed by Western blotting. Lanes 1–4 represent p300 only, p300 + biotinylated Δ^{12}-PGJ$_2$ (1:1 molar ratio), p300 incubated with biotinylated Δ^{12}-PGJ$_2$ and mutant peptide, and p300 incubated with biotinylated Δ^{12}-PGJ$_2$ and wild type peptide, respectively. Since native p300 and p300C1438A were expressed with a GST tag, blots were reprobed with anti-GST to confirm near uniform loading. Representative of $n = 2$ is shown. (C) Mass spectrometric evaluation (by direct infusion) of the interaction of mutant peptide before and after incubation with Δ^{12}-PGJ$_2$.

Figure 7.
Molecular modeling of CyPGs to p300 HAT domain. (A) Predicted precovalent conformers for four PGs in the CoA binding site of p300-HAT. Connolly surface color scheme: hydrophobic = yellow; weakly polar alkyl = white; polar O, N, H = red, blue, and cyan respectively; and the surface of the putatively reactive sulfur on Cys^{1438} = orange for contrast. Ligands are rendered as sticks with CPK colors, except for carbon atoms, which are shown as follows: cocrystallized CoA analogue = white; PGJ_2 = green; Δ^{12}-PGJ_2 = brown; PGK_2 = violet; and 9,10-dihydro-15d-PGJ_2 = black. (B) Docking study of PGs to the p300 HAT domain. (C) Orientation of the cyclopentenone ring of PGs toward Cys^{1438}. (D) Formation of the covalent bond between carbon 9 of CyPG with Cys^{1438} is shown as a dotted line.

Figure 8.
Δ^{12}-PGJ$_2$ inhibits p300-dependent on the acetylation of HIV-1 Tat. (A) rTat was incubated with Δ^{12}-PGJ$_2$ treated and untreated p300 HAT domain and [acetyl-1-^{14}C] CoA. rTat was pulled down using HisPur resin. The resin was washed with PBS, boiled with SDS–PAGE gel loading buffer, and subjected to scintillation counting. Negative and positive controls correspond to p300 + [acetyl-1-^{14}C] CoA and p300 + [acetyl-1-^{14}C] CoA + rTat, respectively. Mean ± SEM values of three independent experiments are shown. (B) U1/HIV cells were stimulated and treated with Δ^{12}-PGJ$_2$ at 2 μM for 24 and 48 h. Day 1, DMSO treated (lane 1), 2 μM Δ^{12}-PGJ$_2$ (lane 2); day 2, DMSO treated (lane 3), 2 μM Δ^{12}-PGJ$_2$ (lane 4). Representative blots of $n = 3$ are shown. (C) Δ^{12}-PGJ$_2$ decreases p24 levels in chronically HIV-1 infected human monocytes. The viral structural protein p24, secreted into the culture medium was estimated by using an antigen-capture assay. The difference between cells treated with the control and 2 μM concentration of Δ^{12}-PGJ$_2$ was found to be statistically significant. Error bars represent the SEM of three independent experiments. *, $p < 0.05$; **, $p < 0.005$. US, unstimulated cells; Veh, vehicle (DMSO).